The Journal of International Advanced Otology

J Int Adv Otol 2025; 21: 1–8 • DOI: 10.5152/iao.2025.241652

Original Article

Analysis of L1 Cell Adhesion Molecule and Fucosyltransferase 8 Expression in Cells After Stretch and Human EACSCC Tissue

Naotaro Akiyama[1,2], Tomomi Yamamoto-Fukuda[2], Hiromi Kojima[2]

[1]Department of Otorhinolaryngology, Tokyo Dental College Ichikawa General Hospital, Ichikawa, Japan
[2]Department of Otorhinolaryngology, Jikei University School of Medicine, Tokyo, Japan

ORCID iDs of the authors: N.A. 0000-0002-2232-2049, T.Y-F. 0000-0002-4168-6315, H.K. 0000-0003-2967-2110.

Cite this article as: Akiyama N, Yamamoto-Fukuda T, Kojima H. Analysis of L1 cell adhesion molecule and fucosyltransferase 8 expression in cells after stretch and human EACSCC tissue. *J Int Adv Otol.* 2025, 21, 1652, doi:10.5152/iao.2025.241652.

BACKGROUND: External auditory canal (EAC) squamous cell carcinoma (SCC) is classified as a rare cancer and has a poor prognosis at advanced stages. Mechanical stress has been implicated in external auditory canal squamous cell carcinoma (EACSCC), but the molecular mechanism has not been elucidated. Mechanotransduction is well-known for Yes-associated protein (YAP) signaling. When YAP is translocated to the nucleus, the L1 cell adhesion molecule (L1CAM) is activated as an effector of mechanotransduction. Core fucosylation of L1CAM by Fucosyltransferase 8 (FUT8) has been implicated in the degree of tumor malignancy, modulating cleavage of the extracellular domain of L1CAM.

METHODS: In this study, an expression analysis of YAP, L1CAM, and FUT8 was performed by stretch assay *in vitro*. Immunohistochemistry was also performed in human EACSCC and normal skin specimens.

RESULTS: The labeling index of FUT8-positive cells exhibited YAP nuclear translocation under stretch stress was significantly higher in a human SCC cell line (HSC1) than in a human keratinocyte cell line. Stretch stress significantly increased the expression levels of full-length L1CAM in HSC1 cells. Moreover, colocalization of FUT8 and L1CAM was demonstrated immunohistochemically in advanced human EACSCC tissues.

CONCLUSION: These results suggested that L1CAM expression is increased under mechanotransduction and may possibly avoid L1CAM cleavage by FUT8 modulation.

KEYWORDS: Mechanotransduction, Yes-associated protein, L1 cell adhesion molecule, fucosyltransferase 8, external auditory canal squamous cell carcinoma

INTRODUCTION

The temporal bone squamous cell carcinoma (SCC) is a rare cancer, accounting for only 0.2% of head and neck SCC (HNSCC).[1,2] Among them, SCC of the external auditory canal (EAC) is the most common, with a relatively good prognosis in the early stages.[1-3] However, external auditory canal squamous cell carcinoma (EACSCC) is characterized by local aggressiveness and has a poor prognosis in the advanced stages.[1-4]

The pathogenesis of EACSCC is unclear but has been suggested to be related to excessive ear touching.[5,6] Mechanotransduction is a biochemical signal that triggers specific cellular responses to mechanical forces.[7,8] Yes-associated protein (YAP) is a transcriptional co-activator that acts as a mechanotransducer.[7,9,10] Under mechanical stress, YAP is translocated to the nucleus in an unphosphorylated state and cooperates with transcription factors to activate many target genes. Yes-associated protein is involved in development and tissue regeneration as well as tumorigenesis, including EACSCC.[7,8,11-13]

In tumorigenesis, the involvement of the L1 cell adhesion molecule (L1CAM) in the activation of YAP has been suggested.[14] L1 cell adhesion molecule is a transmembrane glycoprotein with a molecular weight of 200-220 kDa belonging to the immunoglobulin-like superfamily.[14] The extracellular domain is cleaved and functionally regulated by plasmin and a disintegrin and metalloproteinase.[14,15] L1 cell adhesion molecule plays an essential role in the development of the nervous system but has

Corresponding author: Naotaro Akiyama, e-mail: nakiyama@tdc.ac.jp
Received: July 21, 2024 • **Revision Requested:** July 26, 2024 • **Last Revision Received:** October 19, 2024 • **Accepted:** November 6, 2024 • **Publication Date:** January 27, 2025
Available online at www.advancedotology.org

also been shown to play a critical role in the progression of various tumors.[15-18] Previous reports on the relationship between YAP and L1CAM have shown that L1CAM induces YAP nuclear translocation in tumor cells, activates mechanotransduction signaling, and induces metastasis, and that L1CAM expression increases in a YAP-dependent manner in olfactory ensheathing cells.[11,17] As a direct effect, full-length L1CAM contributes to cell proliferation via MAPK/ERK signaling pathways upon activation of intracellular domains.[19] When L1CAM is cleaved, the soluble cytoplasmic domain promotes gene transcription in an ERK-independent pathway.[19] On the other hand, the extracellular domain of L1CAM is involved in integrin-dependent cancer cell migration and cell survival functions, and this function may be attributed to the extracellular domain of full-length L1CAM or cleaved L1CAM, depending on the cancer cell type.[19,20] Moreover, the upregulation of L1CAM associated with epithelial-to-mesenchymal transition (EMT) is suggested to be related to tumor progression through L1CAM-integrin signaling under mechanotransduction.[21,22]

Glycosylation is one of the post-translational modifications and is classified into N- and O-glycans. Core fucose is an N-glycan structure synthesized by α1,6-fucosyltransferase 8 (FUT8) and is involved in cell adhesion, cell-cell interactions, and various signal transduction.[16,20,23] Recently, FUT8-mediated core fucosylation was shown to increase the degree of tumor malignancy by protecting against cleavage of the extracellular domain of L1CAM.[16,24] However, there have been no reports on FUT8 and the adhesion molecule L1CAM in cells under mechanical stress.

In this study, we investigated the localization and expression levels of YAP, L1CAM, and FUT8 in stretch assays using a normal keratinocyte cell line and a human skin SCC cell line. We also demonstrated immunohistochemical analysis of L1CAM and FUT8 in the EACSCC specimens of T2 as early stage, and T3 and T4 as advanced stages.

METHODS

Cell Culture

A human keratinocyte cell line, human adult low-calcium high-temperature (HaCaT) from the German Cancer Research Center (Deutsches Krebsforschungszentrum; DKF)[25] and human cutaneous SCC cell line, HSC1 (JCRB1015) from the Japanese Collection of Research Bioresources[26] were cultured at 37°C in a humidified atmosphere of 5% CO_2 in air. The cells were cultured with Dulbecco's Modified Eagle's Medium (DMEM) (Thermo Fisher Scientific, Waltham, MA, USA) base medium plus 10% fetal bovine serum (FBS) for HaCaT cells (Sigma-Aldrich, St. Louis, MO, USA) and 20% FBS for HSC1 cells.[25,26]

Cell Stretch Assay

Type I collagen (0.05%) (Cellmatrix Type I-P; Nitta Gelatin Inc., Osaka, Japan) coating was applied to the silicone membrane of the stretch chamber, STB-CH-4W (SC-0044, Strex, Osaka, Japan).[27,28] Then, the cells were plated on the membrane at 4.0×10^4 cells/cm^2 for the HaCaT cells or 2.0×10^4 cells/cm^2 for the HSC1 cells. The cells were allowed to adhere until they reached approximately 70% confluence, and then stretch stress was applied.[25,26] Using a cell stretcher (Strex ST-0100; Strex), traction stress was applied for 2 hours at a 120% traction rate (stretching group, n = 3, each).[10,27,28] In the control group (n = 3, each), traction stress was not applied. With stretch was denoted as (+) and without stretch was denoted as (–).

Patients

The EACSCC cases included 4 males and 2 females with an age range of 35-83 years and a mean age of 55 years. The cases were classified using the University of Pittsburgh tumor, node, metastasis (TNM) staging system for EAC cancer,[29] and treatment, recurrence, secondary treatment, and outcome are summarized in Table 1. Tissues collected from the EACSCC patients who underwent surgery at the Otorhinolaryngology Department of Jikei Hospital between February 2019 and May 2021 were used for analysis. Normal skin taken during surgery was also used as a control for analysis. Pathological diagnoses of the surgical specimens were performed by skilled pathologists. The Human Ethics Review Committee of the Jikei University School of Medicine approved this research protocol (approval number 31-139 9638, date: September 9, 2019). The study was conducted in accordance with the principles of the Declaration of Helsinki after obtaining signatures on the informed consent from all patients or their guardians.

Tissue Preparation

The EACSCC and normal skin specimens were fixed with 4% paraformaldehyde (PFA) in phosphate-buffered saline (PBS), and 5 μm thick serial sections were prepared for analysis. Hematoxylin and eosin (H&E) staining was performed in a standard manner and used for histological analysis.

Immunocytochemistry

Double immunocytostaining was performed as described previously[10,30] to detect the expression of YAP, L1CAM, and FUT8 on the cells on the silicon membrane. Briefly, the cells on the silicon membrane were fixed with 4% PFA in PBS,[10] washed in PBS 3 times,

Table 1. Summary of the External Auditory Canal Squamous Cell Carcinoma Patients

Case	TNM	Stage	Surgical Treatment	Radiation Therapy	Chemotherapy	Recurrence	Secondary Treatment	Survival (□) Death (■)
1	T2N0M0	II	+	+	–	No	–	□
2	T2N0M0	II	+	+	–	No	–	□
3	T3N0M0	III	+	+	–	No	–	□
4	T3N1M0	IV	+	+	+	Yes	CyberKnife	□
5	T4N1M0	IV	+	+	+	–	–	■
6	T4N1M0	IV	+	+	+	–	–	■

TNM, tumor, node, metastasis.

and immersed in 0.1% TritonX-100 (Sigma-Aldrich) in PBS for 5 minutes at room temperature. After blocking with the Blocking One (03953-95, Nacalai Tesque, Kyoto, Japan) for 10 minutes, the cells on the silicon membrane were incubated with the first antibodies: anti-YAP antibody (1 : 200; rabbit; BS1701; Bioworld Technology, St. Louis Park, MN, USA), anti-L1CAM antibody (1 : 200; rabbit; ab208155; Abcam, Cambridge, UK), and anti-FUT8 antibody (1 : 500; mouse; 66118-1-Ig; Proteintech, Rosemont, IL) for 30 minutes at room temperature in a moist chamber. After washing with PBS containing 0.05% Tween 20 (PBST), slides were reacted with secondary antibodies, Alexa Fluor 488-goat anti-mouse IgG (1 : 500; A-11008; Thermo Fisher Scientific) and Alexa Fluor 555-goat anti-rabbit IgG (1 : 500; A-21422; Thermo Fisher Scientific) for 30 minutes. 4′,6-diamidino-2-phenylindole (DAPI) was used for counterstaining and visualized with a fluorescence conjugate. For a negative control, normal mouse IgG (1 : 500) and normal rabbit IgG (1 : 200) were used instead of the first antibodies in every experiment.

Immunohistochemistry

Enzyme immunohistochemistry was demonstrated to detect L1CAM in paraffin sections of EACSCC.[10] After deparaffinization and rehydration of the paraffin sections, the high temperature antigen retrieval method at 120°C for 10 minutes in Tris/EDTA buffer (pH 9.0) was performed. To block nonspecific reactions, slides were preincubated with Blocking One for 10 minutes at room temperature and then incubated with anti-L1CAM antibody (1 : 200; rabbit; EPR18750; Abcam) overnight. After washing with PBST, reaction with the horseradish peroxidase (HRP)-anti-rabbit antibody was performed. Visualization was performed using a mixture containing diaminobenzidine and H_2O_2 against the horseradish peroxidase sites. Normal rabbit IgG diluted to 1 : 200 was used instead of the primary antibody as a negative control. Double immunohistostaining was also performed as described previously[30,31] to detect the expression of L1CAM and FUT8 on the EACSCC or normal-skin specimens. After deparaffinization and rehydration, the antigen retrieval was performed by autoclaving in HistoVT One (Nacalai Tesque) at 90°C for 20 minutes. The slides were then preincubated with Blocking One for 10 minutes at room temperature to block nonspecific reactions and were incubated with anti-L1CAM antibody (1 : 200; rabbit; ab208155; Abcam) and anti-FUT8 antibody (1 : 400; mouse; 66118-1-Ig; Proteintech) overnight. After being washed with PBST, the slides were immersed with the secondary antibodies, Alexa Fluor 488-goat anti-mouse IgG (1 : 500; A-11008; Thermo Fisher Scientific) and Alexa Fluor 555-goat anti-rabbit IgG (1 : 500; A-21422; Thermo Fisher Scientific) at 4°C for 60 minutes. After washing with PBST and DAPI counterstaining, visualization by fluorescence conjugate was performed. Normal mouse IgG diluted to 1 : 400 or rabbit IgG diluted to 1 : 200 was immersed as a negative control.

Western Blotting

Western-blot analyses were performed as described in previous reports.[30,32] About 2.0×10^5 cells were lysed with 2× Laemmli buffer (Bio-Rad, Hercules, CA, USA), 2-mercaptoethanol, and protein/phosphatase inhibitor (Cell Signaling Technology, Danvers, MA, USA). The protein samples were separated in precast polyacrylamide gels (Thermo Fisher Scientific) by electrophoresis and transferred to the polyvinylidene difluoride (PVDF) membranes using the iBlot 2 Transfer Stacks (Life Technologies). The PVDF membranes were incubated with 5% nonfat dry milk (#9999, Cell Signaling Technology) in 0.1% Tween 20 in Tris-buffered saline for 60 minutes and immersed with anti-β-actin antibody diluted to 1 : 2000 (rabbit; #4970; Cell Signaling Technology), anti-YAP antibody diluted to 1 : 500 (rabbit; BS1701; Bioworld Technology), anti-FUT8 antibody diluted to 1 : 2000 (mouse; 66118-1-Ig; Proteintech), or anti-L1CAM antibody diluted to 1 : 500 (mouse; ab20148; Abcam). The complexes of target antigen and primary antibody were detected using HRP goat anti-mouse IgG (#7076; Cell Signaling Technology) or HRP goat anti-rabbit IgG (#7074; Cell Signaling Technology) diluted to 1 : 10 000 for 60 minutes. The PVDF membranes were stripped using WB Stripping Solution (Nacalai Tesque) and the same membrane was used for anti-YAP antibody, anti-FUT8 antibody, and loading control β-actin. The other membrane was stripped using WB Stripping Solution and was used for anti-L1CAM antibody and loading control β-actin. The signals were detected by the ECL Western blotting detection system (ECL Prime; GE Healthcare, Chicago, IL, USA) and the protein bands were imaged by LAS-4000 luminescent image analyzer (Fujifilm, Tokyo, Japan).

Microscopy, Imaging Analysis Software and Cell Counting Measurement

Images of the H&E staining sections and the enzyme-immunohistochemical staining sections were captured by an Axio Cam camera and analyzed using AxioVision software version 4.8 (Carl Zeiss, Jena, Germany). Fluorescent images were captured using Zeiss LSM 880 confocal microscope systems and analyzed by ZEN microscopy software (ZEN 2.1 black edition). For the analysis of immunofluorescence staining of YAP and FUT8 in the stretch assay, DAPI labeling was used to account for the total number of cells, and 3 10 000 μm^2 (100 × 100 μm squares) areas per sample were used as equal areas at ×400. To clarify the colocalization of L1CAM and FUT8 in EACSCC specimens, 0.5 mm z-stack images of each section were acquired using LSM880.[10] Quantification of Western blot bands was analyzed using ImageJ (version 15.1, NIH, Bethesda, MD; https://imagej.nih.gov/ij).[33]

Statistical Analysis

The percentage of positive cells to the total number of cells was expressed as a labeling index (LI), mean ± standard deviation. For Western blotting analysis, signal intensities were calculated using β-actin as a loading control. For normally distributed data, one-way analysis of variance (ANOVA) tests and Tukey post hoc tests were used to examine the statistical significance of differences between groups. A *P*-value of less than .05 denoted a statistically significant difference. All data were analyzed using JMP software version 13 (SAS Institute Japan; Tokyo, Japan).

RESULTS

The Expression of YAP and FUT8 in HaCaT Cells and HSC1 Cells After Uniaxial Stretch

Immunocytochemistry was performed after uniaxial stretch of the HaCaT cells and HSC1 cells using anti-YAP and anti-FUT8 antibodies. Cells that were not stretch-stressed were used as controls. As a result, stretch stress-induced YAP nuclear translocation in both HaCaT cells and HSC1 cells (HaCaT [−]: 1.50 ± 0.17; HaCaT [+]: 13.59 ± 1.42; HSC1 [−]: 2.66 ± 0.25; HSC1 [+]: 15.82 ± 1.56; n = 3, each; HaCaT [−] vs. HaCaT [+]: $P < .0001$; HaCaT [−] vs. HSC1 [+]: $P < .0001$; HSC1 [−] vs. HSC1 [+]: $P < .0001$; HSC1 [−] vs. HaCaT [+]: $P < .0001$) (Figure 1A

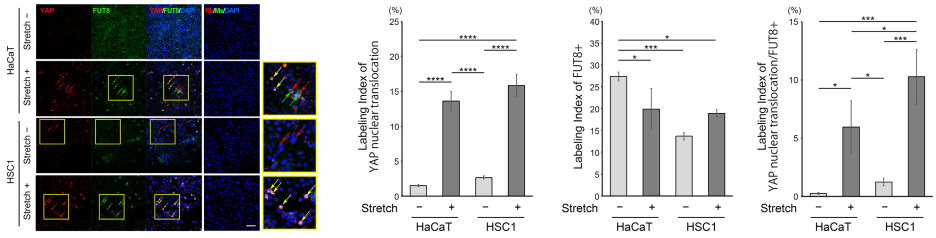

Figure 1. Immunocytochemistry of Yes-associated protein (YAP) and Fucosyltransferase 8 (FUT8) in stretch assays of HaCaT and HSC1 cells. A. Double immunofluorescence staining of YAP (red) and FUT8 (green). The nuclei were stained with 4′,6-diamidino-2-phenylindole (DAPI) (blue). From top to bottom: HaCaT cells without stretch stress (–), HaCaT cells with stretch stress (+), HSC1 (–), and HSC1 (+). Yes-associated protein nuclear translocation was increased in both in HaCaT cells and HSC1 cells with stretch stress. In the absence of stretch stress, FUT8 was expressed in the cytoplasm, with expression levels higher in HaCaT cells than in HSC1 cells. Cytoplasmic FUT8 expression levels were increased in some HaCaT (+) and HSC1 (+). Red arrows: YAP-positive cells; green arrows: FUT8 highly positive cells; yellow arrows: YAP nuclear-translocated and FUT8-positive cells. Insets: high-power view. Scale bars: 100 µm. B. Labeling index (LI) of YAP nuclear translocation (Left). LI of FUT8-positive cells (middle). LI of YAP nuclear-translocated and FUT8 positive cells (right). All data are expressed relative expressions as means ± SD. n = 3 each. *P < .05, ***P < .001, ****P < .0001 (one-way analysis of variance test, followed by the Tukey post hoc tests for normally distributed data).

and B). In the absence of stretch stress, FUT8 was expressed in the cytoplasm diffusely, with the high LI of FUT8 in HaCaT cells than in HSC1 cells (Figure 1A and B). On the other hand, the LI of FUT8 was not increased both in HSC1 and in HaCaT cells when stretch stress was applied, but each FUT8 expression signal was enhanced (HaCaT [–]: 27.35 ± 0.99; HaCaT [+]: 19.88 ± 4.72; HSC1 [–]: 13.65 ± 0.85; HSC1 [+]: 18.93 ± 0.82; n = 3, each; HaCaT [–] vs. HaCaT [+]: P < .05; HaCaT [–] vs. HSC1 [–]: P < .001; HaCaT [–] vs. HSC1 [+]: P < .05) (Figure 1A and B). The nuclear translocation of YAP was confirmed in a greater number of HSC1 cells after stretch, and those cells were FUT8 positive, while cytoplasmic YAP-positive signals were strong in HSC1 without stretch stress (Figure 1A and B). These results indicated that HSC1 cells were more susceptible to mechanical stress than HaCaT cells, further suggesting that a large number of YAP nuclear transition cells may be FUT8-positive cells. In fact, compared to HaCaT cells, HSCs showed a higher rate of increase in LI of YAP nuclear-translocated and FUT8-positive cells with stretch stress compared with those without stretch stress (HaCaT [–]: 0.26 ± 0.07; HaCaT [+]: 6.53 ± 2.28; HSC1 [–]: 1.24 ± 0.31; HSC1 [+]: 10.28 ± 2.37; n = 3, each; HaCaT [–] vs. HaCaT [+]: P < .05; HSC1 [–] vs. HSC1 [+]: P < .001) (Figure 1B). Furthermore, the LI of YAP nuclear-translocated and FUT8-positive cells in HSC1 (+) was significantly increased compared with HaCaT (+) (HaCaT [+] vs. HSC1 [+]: P < .05) (Figure 1B).

The Expression of L1CAM and FUT8 in HaCaT Cells and HSC1 Cells After Uniaxial Stretch

Next, immunocytochemistry was performed after uniaxial stretch of the HaCaT cells and HSC1 cells using anti-L1CAM and anti-FUT8 antibodies. Cells that were not stretch-stressed were used as controls. As a result, L1CAM was slightly expressed in HaCaT cells, but some of them were colocalized with L1CAM and upregulated in HSC1 cells (Figure 2, red arrows). Furthermore, in HSC1 cells, many cells were found to be single positive for L1CAM without stretch stress, while L1CAM and FUT8 were mostly co-localized when stretch stress was applied (Figure 2, yellow arrows).

Western Blotting Analysis of YAP, FUT8, and L1CAM in HaCaT Cells and HSC1 Cells After Uniaxial Stretch

Western blotting was performed after the uniaxial stretch of the HaCaT cells and HSC1 cells. Cells without stretch were used as controls. The results showed that stretch stress significantly increased YAP expression levels in HaCaT cells compared to controls. (HaCaT [–]: 0.23 ± 0.07; HaCaT [+]: 0.50 ± 0.09; HSC1 [–]: 0.53 ± 0.13; HSC1 [+]: 0.54 ± 0.05; n = 3, each; HaCaT [–] vs. HaCaT [+]: P < .05) (Figure 3A and B). The expression level of FUT8 was decreased in HaCaT cells compared to controls but significantly increased in HSC1 cells. (HaCaT [–]: 0.99 ± 0.13; HaCaT [+]: 0.44 ± 0.10; HSC1 [–]: 0.21 ± 0.01; HSC1 [+]: 0.47 ± 0.03; n = 3, each; HaCaT [–] vs. HaCaT [+]: P < .001; HSC1 [–] vs. HSC1 [+]: P < .05) (Figure 3A and C). When analyzed for L1CAM, the expression levels were low in the HaCaT cells and did not change after stretching (Figure 3D-F). On the other hand, full-length L1CAM expression levels were increased in HSC1 cells and were further upregulated by stretch stress (HaCaT [–]: 0.26 ± 0.05; HaCaT [+]: 0.33 ± 0.05; HSC1 [–]: 2.09 ± 0.54; HSC1 [+]: 3.59 ± 0.54; n = 3, each; HSC1 [–] vs. HSC1 [+]: P < .05; HaCaT [+] vs. HSC1 [–]: P < .05; HaCaT [–] vs. HSC1 [–]: P < .05; HaCaT [+] vs. HSC1 [+]: P < .001; HaCaT [–] vs. HSC1 [+]: P < .01) (Figure 3D and E). In addition, the expression levels of cleaved L1CAM in HSC1 cells were not increased by stretch stress (HaCaT [–]: 0.03 ± 0.01; HaCaT [+]: 0.01 ± 0.01; HSC1

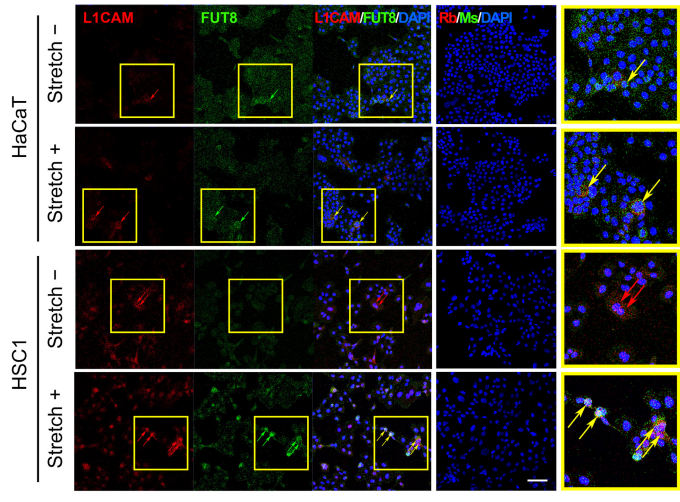

Figure 2. Immunocytochemistry of L1 cell adhesion molecule (L1CAM) and Fucosyltransferase 8 (FUT8) in stretch assays of HaCaT and HSC1 cells. Double immunofluorescence staining of L1CAM (red) and FUT8 (green). The nuclei were stained with 4′,6-diamidino-2-phenylindole (DAPI) (blue). From top to bottom: HaCaT cells without stretch stress (–), HaCaT cells with stretch stress (+), HSC1 (–), and HSC1 (+). L1CAM was highly expressed in HSC1 cells and co-localized with FUT8 via stretch stress. Red arrows: L1CAM-positive cells; green arrows: FUT8-highly positive cells; yellow arrows: double-positive cells. Insets: High-power view. Scale bars: 100 µm.

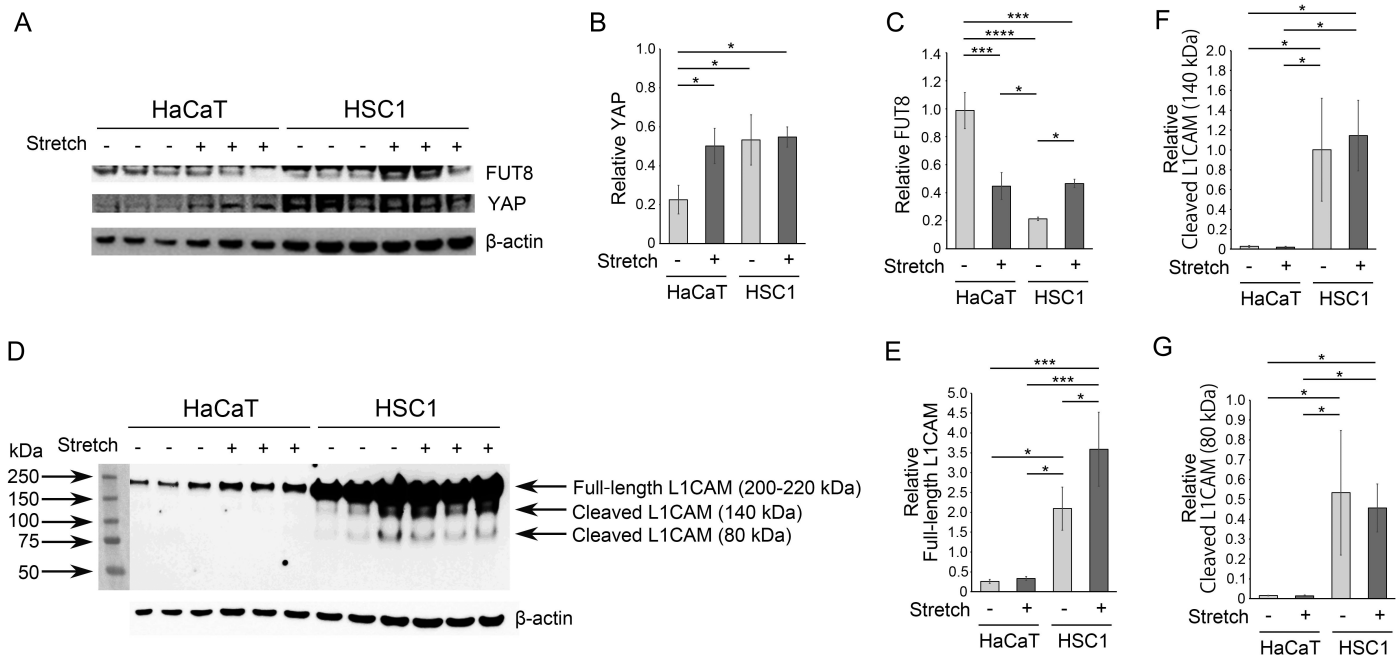

Figure 3. Western blotting of Yes-associated protein (YAP), L1 cell adhesion molecule (L1CAM), and Fucosyltransferase 8 (FUT8) in stretch assays of HaCaT and HSC1 cells. A-C. Western blotting analysis of YAP (65 kDa) and FUT8 (66 kDa) protein levels in HaCaT cells (left lanes) and HSC1 cells (right lanes) with (+) or without (–) stretch stress. β-actin (45 kDa) was used as a loading control (A). The relative protein levels of YAP in the HaCaT and HSC1 cells with (+) or without (–) stretch stress (B). The relative protein levels of FUT8 in the HaCaT and HSC1 cells with (+) or without (–) stretch stress (C). D-G. Western blotting analysis of L1CAM protein levels in HaCaT cells (left lanes) and in HSC1 cells (right lanes) with (+) or without (–) stretch stress (200–220 kDa, full-length L1CAM; 140 kDa, cleaved L1CAM; 80 kDa, cleaved L1CAM; 45 kDa, β-actin) (D). The relative protein levels of full-length L1CAM in HaCaT cells (left lanes) and HSC1 cells (right lanes) with (+) or without (–) stretch stress (E). The relative protein levels of cleaved L1CAM in HaCaT cells (left lanes) and HSC1 cells (right lanes) with (+) or without (–) stretch stress (F, G). The level of β-actin was used as a loading control. All data are expressed relative expressions as means ± SD. n = 3 each. **P* < .05, ****P* < .001, *****P* < .0001 (one-way analysis of variance test, followed by the Tukey post hoc tests for normally distributed data).

[–]: 1.00 ± 0.52; HSC1 [+]: 1.14 ± 0.35; n = 3, Cleaved L1CAM [140 kDa], each, HaCaT [–]: 0.02 ± 0.00; HaCaT [+]: 0.01 ± 0.00; HSC1 [–]: 0.53 ± 0.31; HSC1 [+]: 0.45 ± 0.12; n = 3, Cleaved L1CAM [80 kDa], each) (Figure 3D,F,G).

Immunohistochemical Analysis of Human EACSCC Specimens

Finally, an immunohistochemical analysis of L1CAM and FUT8 was performed for the EACSCC and normal skin tissues. The summary of EACSCC patients is listed in Table 1. The expression levels of L1CAM and FUT8 were increased in the EACSCC tissues compared to the normal skin tissues (Figure 4A and B). In cases 1 and 2 of T2, and case 3 of T3, L1CAM and FUT8 were not colocalized; in case 4 of T3, L1CAM and FUT8 were colocalized; and in cases 5 and 6 of T4, double-positive cells increased (Figure 4A). The z-stack images revealed the colocalization of L1CAM and FUT8 in cases 4, 5, and 6 (Figure 4A, yellow arrows).

DISCUSSION

In this study, the expression levels of YAP, L1CAM, and FUT8 were evaluated concerning mechanotransduction in EACSCC. Stretch assays were conducted with a human keratinocyte cell line, HaCaT cells, and a human cutaneous SCC cell line, HSC1 cells.

As a result of the immunocytochemistry, YAP nuclear translocation was increased after stretch stress in HaCaT cells and HSC1 cells, confirming mechanotransduction in both cell lines. Western blotting analysis revealed a significant increase in the expression levels of YAP in HaCaT cells with stretch stress compared with those without stretch stress. Interestingly, the expression levels of YAP in HSC1 cells were significantly elevated in the pre-stretch phase compared to pre-stretch HaCaT cells and were further elevated after stretching. This is consistent with previous findings that cytoplasmically localized YAP is phosphorylated and degraded, but its expression is elevated in proliferative diseases, suggesting that it is prepared for nuclear recruitment.[9] As expected, HSC1 cells appeared to be more sensitive to mechanical stimulation than HaCaT cells, a result consistent with previous reports.[34] These results indicate that SCC cells might be more sensitive to mechanical stress than normal cells.

In many cancers, glycosylation has been implicated in tumor invasion and metastasis.[24] Recently, the importance of core fucosylation by FUT8 has been demonstrated in colorectal cancer, non-small cell lung cancer, breast cancer, glioblastoma, and melanoma.[16,24] In this study, immunocytochemical analysis showed that FUT8 was diffusely expressed in the cytoplasm of HaCaT cells. Under stretch stress, the FUT8 LI decreased, although the FUT8-positive signal was enhanced. On the other hand, in HSC1 cells, FUT8 expression was low without stretch stress, but stretch stress enhanced FUT8-positive signals. Furthermore, Western blotting analysis confirmed the significant upregulation of FUT8 after stretching in HSC1 cells. Double staining for YAP and FUT8 revealed that cells exhibiting YAP nuclear translocation and FUT8 expression significantly increased by stretch stress in HSC1 cells. In other words, HSC1 cells were suggested to be more susceptible to stretch stress-induced core fucosylation by FUT8 than HaCaT cells. Furthermore, stretch stress increased FUT8 expression in HSC1 cells. This core fucosylation by FUT8 has been suggested to be

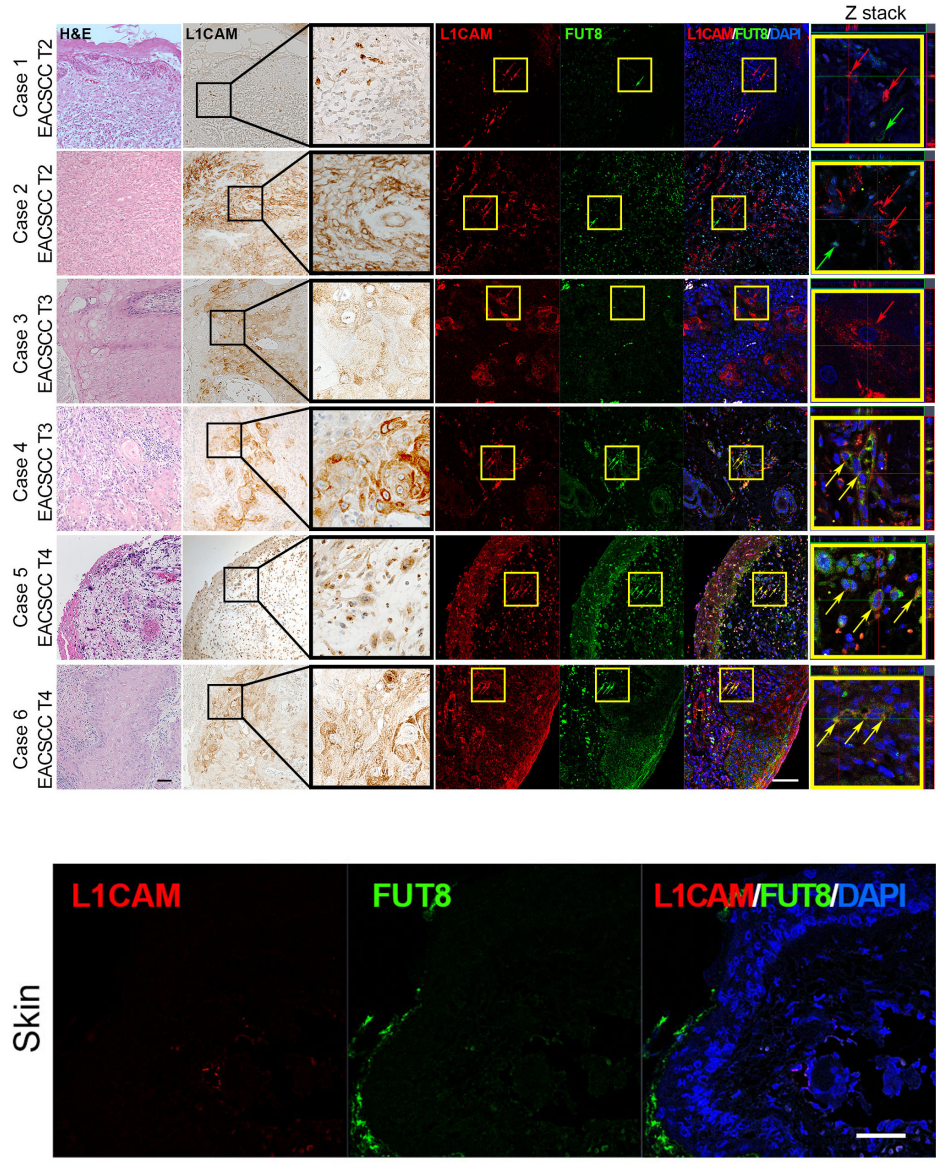

Figure 4. Immunohistochemistry of L1 cell adhesion molecule (L1CAM) and Fucosyltransferase 8 (FUT8) in sections of the external auditory canal squamous cell carcinoma (EACSCC) and normal skin specimens. A. Hematoxylin and eosin (H&E) staining of the EACSCC specimens, enzyme immunohistochemistry of L1CAM, and double immunofluorescence staining of L1CAM (red) and FUT8 (green). Nuclei were counter-stained with 4′,6-diamidino-2-phenylindole (DAPI) (blue) for immunofluorescence staining. From top to bottom: cases 1 and 2 of EACSCC T2, cases 3 and 4 of EACSCC T3, and cases 5 and 6 of EACSCC T4. A summary of the patients of EACSCC is listed in Table 1. Enzyme immunohistochemistry of L1CAM showed positive signals in the plasma membrane of cancer cells. Colocalization of L1CAM and FUT8 (yellow) was rarely observed in cases 1, 2, and 3, and the number of L1CAM (+)/FUT8 (+) cells increased as the T phase progressed. B. L1CAM (red) and FUT8 (green) expression were low in the normal skin specimen. Red arrows: L1CAM-positive cells; green arrows: FUT8-positive cells; Yellow arrows: double-positive cells. The black boxed area corresponds to the high-power view of the enzyme immunohistochemistry of L1CAM. The yellow boxed area corresponds to the high-power view with z-stack images, orthogonal display, xy, yz, and xz options shown to the right. Scale bars: 50 µm.

associated with invasive and metastatic potential in many cancers,[35] and HSC1 cells may have increased invasive and metastatic potential due to stretch stress.

Full-length L1CAM consists of a long ectodomain that comprises 6 immunoglobulin-like domains followed by 5 fibronectin type III repeats, a transmembrane domain and an intracellular domain (Figure 5).[19] Functional diversity of L1CAM and its fragments has been reported in the developing and diseased nervous system, as well as in some solid tumors, but the mechanisms are not fully understood.[18-20] Recent studies have revealed that FUT8-mediated core fucosylation increases tumor invasiveness and metastasis by evading cleavage of the extracellular domain of L1CAM.[16] In fact, stretch assays of HSC1 cells revealed increased expression levels of FUT8 and significant upregulation of full-length L1CAM in Western blotting analysis. Unexpectedly, however, the expression of cleaved L1CAM in HSC1 cells was reduced relative to that of full-length L1CAM under stretch stress, but the expression levels of cleaved L1CAM detected in unstretched HSC1 cells (80 kDa or 140 kDa) did not decrease after stretch (Figure 3D, F, G). Previous reports have suggested that cleaved L1CAM is associated with cancer invasion and metastasis. Indeed, cleaved L1CAM was barely expressed in HaCaT cells, whereas its expression was elevated in HSC1 cells even in the pre-stretch stress state (Figure 3D, F, G). The expression of full-length

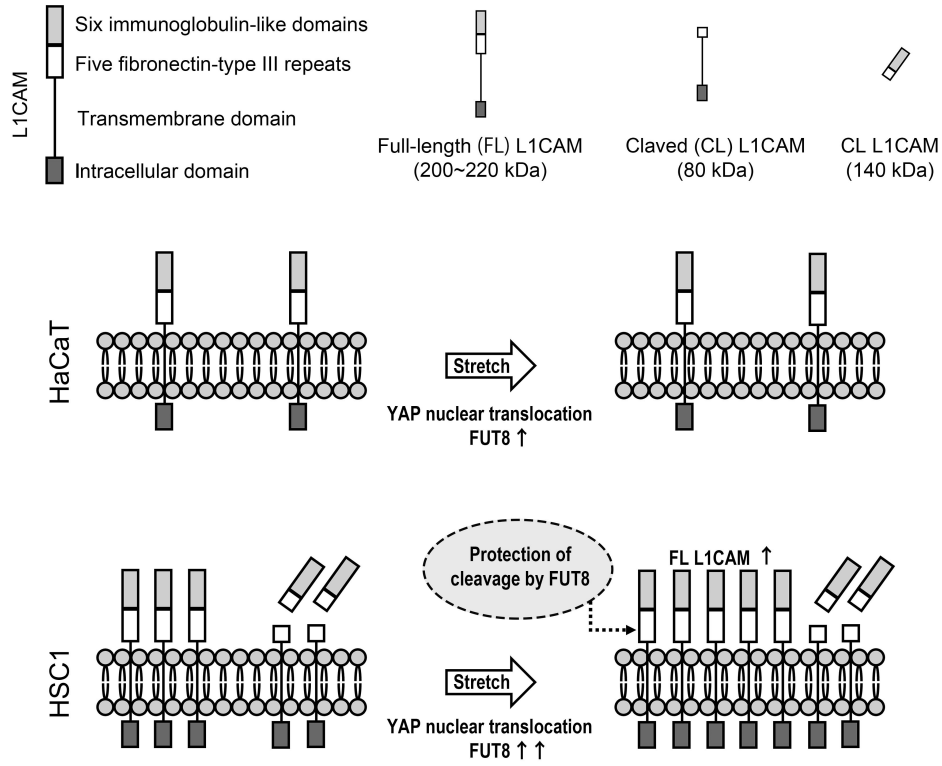

Figure 5. Structure of L1CAM and a summary schema of the relationship between YAP, FUT8, and L1CAM in this study. Full-length L1CAM consists of a long ectodomain that comprises 6 immunoglobulin-like domains followed by 5 fibronectin type III repeats, a transmembrane domain and an intracellular domain. The molecular weight of L1CAM is 220-200 kDa, and the cleaved L1CAMs detected in this study were 140 kDa and 80 kDa. Stretch stress induces YAP nuclear translocation under stretch stress. After stretch stress, FUT8 is highly elevated in a human SCC cell line (HSC1) compared to a human keratinocyte cell line (HaCaT). Stretch stress induces higher L1CAM expression in HSC1 cells compared to HaCaT cells, suggesting that FUT8 may be involved in evading L1CAM cleavage and increasing full-length L1CAM.

L1CAM and cleaved L1CAM was significantly elevated in HSC1 cells compared to that in HaCaT cells with or without stretch stress (Figure 3D and E). These results suggest that both full-length L1CAM and cleaved L1CAM may be involved in a cell-specific function in HSC1 cells (Figure 5).

Finally, immunohistochemistry in the EACSCC and normal skin specimens was performed. In EACSCC, T classification often reflects the stage of the disease. Interestingly, the colocalization of L1CAM and FUT8 was more pronounced in more advanced the T classifications immunohistochemically, although the expression levels were low in the normal skin specimens. Morphologically, relatively highly differentiated cells tended to show little colocalization of L1CAM and FUT8, while relatively undifferentiated cells that did not show cell polarity tended to show colocalization of L1CAM and FUT8. It has been reported that L1CAM is highly expressed in invasive cancer cells and correlates with malignancy, suggesting an association with EMT.[21,22] In the EMT of invasive cancer cells, L1CAM-integrin signaling, i.e., outside-in signaling such as mechanosensing through the extracellular domain of L1CAM, is considered important.[21] The increase in full-length L1CAM in HSC1 cells under stretch stress may include the EMT process via mechanotransduction. In addition, the increased colocalization of L1CAM and FUT8 in advanced human EACSCC specimens suggests that the core fucosylation of L1CAM in EACSCC may avoid further L1CAM cleavage. However, the number of cases studied is small, so a large-scale analysis should be added in the future.

Availability of Data and MaterialsStatement: The data that support the findings of this study are available from the corresponding author, N. A., upon reasonable request.

Ethics Committee Approval: This study was approved by the Ethics Committee of Jikei University (approval no.: 31-139 9638, date: September 09, 2019).

Informed Consent: Written informed consent was obtained from the patients who agreed to take part in the study.

Peer-review: Externally peer-reviewed.

Author Contributions: Concept – N.A.; Designhelp_outline – N.A., T.YF.; Supervision – T.YF.; Resources – N.A., T.YF.; Materials – N.A., T.YF.; Data Collection and/or Processing – N.A., T.YF.; Analysis and/or Interpretation – N.A., T.YF.; Literature Search – N.A.; Writing – N.A.; Critical Review – N.A., T.YF., H.K.

Declaration of Interests: The authors have no conflicts of interest to declare.

Acknowledgments: The authors would like thank Yukio Nishiya, Masahiro Takahashi, Yukihisa Harayama, Eiji Shimura, Takanori Hama, and Yutaka Yamamoto (Department of Otorhinolaryngology, Jikei University School of Medicine) for the harvesting of human tissues; Hiroyuki Takahashi (Department of Pathology, Jikei University School of Medicine) for the pathological diagnoses in this work.

Funding: This study is supported by a Grant-in-Aid for Scientific Research from the Japanese Society for the Promotion of Science (JSPS) (no. JP18K16908

and 22K09754 to N. Akiyama, no. JP19K09857 and 22K09753 to T. Yamamoto-Fukuda).

REFERENCES

1. Lovin BD, Gidley PW. Squamous cell carcinoma of the temporal bone: a current review. *Laryngoscope Investig Otolaryngol*. 2019;4(6):684-692. [CrossRef]
2. Lechner M, Sutton L, Murkin C, et al. Squamous cell cancer of the temporal bone: a review of the literature. *Eur Arch Otorhinolaryngol*. 2021;278(7):2225-2228. [CrossRef]
3. Akiyama N, Yamamoto-Fukuda T, Kojima H. miR-34a predicts the prognosis of advanced-stage external auditory canal squamous cell carcinoma. *Acta Otolaryngol*. 2022;142(6):537-541. [CrossRef]
4. Akiyama N, Yamamoto-Fukuda T, Yoshikawa M, Kojima H. Analysis of the epidermal growth factor receptor/phosphoinositide-dependent protein kinase-1 axis in tumor of the external auditory canal in response to epidermal growth factor stimulation. *Laryngoscope Investig Otolaryngol*. 2022;7(3):730-739. [CrossRef]
5. Hobson JC, Lavy JA. Use and abuse of cotton buds. *J R Soc Med*. 2005;98(8):360-361. [CrossRef]
6. Tsunoda A, Sumi T, Terasaki O, Kishimoto S. Right dominance in the incidence of external auditory canal squamous cell carcinoma in the Japanese population: does handedness affect carcinogenesis? *Laryngoscope Investig Otolaryngol*. 2017;2(1):19-22. [CrossRef]
7. Panciera T, Azzolin L, Cordenonsi M, Piccolo S. Mechanobiology of YAP and TAZ in physiology and disease. *Nat Rev Mol Cell Biol*. 2017;18(12):758-770. [CrossRef]
8. Bansaccal N, Vieugue P, Sarate R, et al. The extracellular matrix dictates regional competence for tumour initiation. *Nature*. 2023;623(7988):828-835. [CrossRef]
9. Akiyama N, Yamamoto-Fukuda T, Yoshikawa M, Kojima H. Evaluation of YAP signaling in a rat tympanic membrane under a continuous negative pressure load and in human middle ear cholesteatoma. *Acta Otolaryngol*. 2017;137(11):1158-1165. [CrossRef]
10. Yamamoto-Fukuda T, Akiyama N, Kojima H. L1CAM-ILK-YAP mechanotransduction drives proliferative activity of epithelial cells in middle ear cholesteatoma. *Am J Pathol*. 2020;190(8):1667-1679. [CrossRef]
11. Er EE, Valiente M, Ganesh K, et al. Pericyte-like spreading by disseminated cancer cells activates YAP and MRTF for metastatic colonization. *Nat Cell Biol*. 2018;20(8):966-978. [CrossRef]
12. Basura GJ, Smith JD, Ellsperman S, Bhangale A, Brenner JC. Targeted molecular characterization of external auditory canal squamous cell carcinomas. *Laryngoscope Investig Otolaryngol*. 2021;6(5):1151-1157. [CrossRef]
13. Driskill JH, Pan D. Control of stem cell renewal and fate by YAP and TAZ. *Nat Rev Mol Cell Biol*. 2023;24(12):895-911. [CrossRef]
14. Moos M, Tacke R, Scherer H, Teplow D, Früh K, Schachner M. Neural adhesion molecule L1 as a member of the immunoglobulin superfamily with binding domains similar to fibronectin. *Nature*. 1988;334(6184):701-703. [CrossRef]
15. Kiefel H, Bondong S, Hazin J, et al. L1CAM: a major driver for tumor cell invasion and motility. *Cell Adh Migr*. 2012;6(4):374-384. [CrossRef]
16. Agrawal P, Fontanals-Cirera B, Sokolova E, et al. A systems biology approach identifies FUT8 as a driver of melanoma metastasis. *Cancer Cell*. 2017;31(6):804-819.e7. [CrossRef]
17. Li Y, Huo S, Fang Y, et al. ROCK Inhibitor Y27632 induced morphological shift and enhanced neurite outgrowth-promoting property of olfactory ensheathing cells via YAP-dependent up-regulation of L1-CAM. *Front Cell Neurosci*. 2018;12:489. [CrossRef]
18. Giordano M, Decio A, Battistini C, et al. L1CAM promotes ovarian cancer stemness and tumor initiation via FGFR1/SRC/STAT3 signaling. *J Exp Clin Cancer Res*. 2021;40(1):319. [CrossRef]
19. Maten MV, Reijnen C, Pijnenborg JMA, Zegers MM. L1 cell adhesion molecule in cancer, a systematic review on domain-specific functions. *Int J Mol Sci*. 2019;20(17):4180. [CrossRef]
20. Chien MH, Yang YC, Ho KH, et al. Cyclic increase in the ADAMTS1-L1CAM-EGFR axis promotes the EMT and cervical lymph node metastasis of oral squamous cell carcinoma. *Cell Death Dis*. 2024;15(1):82. [CrossRef]
21. Kiefel H, Bondong S, Pfeifer M, et al. EMT-associated up-regulation of L1CAM provides insights into L1CAM-mediated integrin signalling and NF-κB activation. *Carcinogenesis*. 2012;33(10):1919-1929. [CrossRef]
22. Altevogt P, Ben-Ze'ev A, Gavert N, Schumacher U, Schäfer H, Sebens S. Recent insights into the role of L1CAM in cancer initiation and progression. *Int J Cancer*. 2020;147(12):3292-3296. [CrossRef]
23. Tomida S, Takata M, Hirata T, Nagae M, Nakano M, Kizuka Y. The SH3 domain in the fucosyltransferase FUT8 controls FUT8 activity and localization and is essential for core fucosylation. *J Biol Chem*. 2020;295(23):7992-8004. [CrossRef]
24. Thomas D, Rathinavel AK, Radhakrishnan P. Altered glycosylation in cancer: a promising target for biomarkers and therapeutics. *Biochim Biophys Acta Rev Cancer*. 2021;1875(1):188464. [CrossRef]
25. Boukamp P, Petrussevska RT, Breitkreutz D, Hornung J, Markham A, Fusenig NE. Normal keratinization in a spontaneously immortalized aneuploid human keratinocyte cell line. *J Cell Biol*. 1988;106(3):761-771. [CrossRef]
26. Kondo S, Aso K. Establishment of a cell line of human skin squamous cell carcinoma in vitro. *Br J Dermatol*. 1981;105(2):125-132. [CrossRef]
27. Kurita M, Okazaki M, Fujino T, Takushima A, Harii K. Cyclic stretch induces upregulation of endothelin-1 with keratinocytes in vitro: possible role in mechanical stress-induced hyperpigmentation. *Biochem Biophys Res Commun*. 2011;409(1):103-107. [CrossRef]
28. Iwata M, Hayakawa K, Murakami T, et al. Uniaxial cyclic stretch-stimulated glucose transport is mediated by a Ca-dependent mechanism in cultured skeletal muscle cells. *Pathobiology*. 2007;74(3):159-168. [CrossRef]
29. Moody SA, Hirsch BE, Myers EN. Squamous cell carcinoma of the external auditory canal: an evaluation of a staging system. *Am J Otol*. 2000;21(4):582-588.
30. Yamamoto-Fukuda T, Akiyama N, Tatsumi N, Okabe M, Kojima H. Keratinocyte growth factor stimulates growth of p75+ neural crest lineage cells during middle ear cholesteatoma formation in mice. *Am J Pathol*. 2022;192(11):1573-1591. [CrossRef]
31. Akiyama N, Yamamoto-Fukuda T, Yoshikawa M, Kojima H. Regulation of DNA methylation levels in the process of oral mucosal regeneration in a rat oral ulcer model. *Histol Histopathol*. 2020;35(3):247-256. [CrossRef]
32. Yamamoto-Fukuda T, Akiyama N, Kojima H. Super-enhancer acquisition drives FOXC2 expression in middle ear cholesteatoma. *J Assoc Res Otolaryngol*. 2021;22(4):405-424. [CrossRef]
33. Schneider CA, Rasband WS, Eliceiri KW. NIH Image to ImageJ: 25 years of image analysis. *Nat Methods*. 2012;9(7):671-675. [CrossRef]
34. Suresh S. Biomechanics and biophysics of cancer cells. *Acta Biomater*. 2007;3(4):413-438. [CrossRef]
35. Bastian K, Scott E, Elliott DJ, Munkley J. FUT8 alpha-(1,6)-fucosyltransferase in cancer. *Int J Mol Sci*. 2021;22(1):455. [CrossRef]